

Experimental Observation of Simultaneous Wave and Particle Behaviors in a Narrowband Single Photon's Wave Packet

Hui Yan,^{1,*} Kaiyu Liao,¹ Zhitao Deng,¹ Junyu He,¹ Zheng-Yuan Xue,¹ Zhi-Ming Zhang,² and Shi-Liang Zhu^{3,1,†}

¹*Laboratory of Quantum Engineering and Quantum Materials,
School of Physics and Telecommunication Engineering,
South China Normal University, Guangzhou 510006, China*

²*Laboratory of Quantum Engineering and Quantum Materials,
School of Information and Photoelectronic Science and Engineering,
South China Normal University, Guangzhou 510006, China*

³*National Laboratory of Solid State Microstructures,
School of Physics, Nanjing University, Nanjing 210093, China*

Light's wave-particle duality is at the heart of quantum mechanics and can be well illustrated by Wheeler's delayed-choice experiment. The choice of inserting or removing the second classical (quantum) beam splitter in a Mach-Zehnder interferometer determines the classical (quantum) wave-particle behaviors of a photon. In this paper, we report our experiment using the classical beam splitter to observe the simultaneous wave-particle behaviors in the wave-packet of a narrowband single photon. This observation suggests that it is necessary to generalize the current quantum wave-particle duality theory. Our experiment demonstrates that the produced wave-particle state can be considered an additional degree of freedom and can be utilized in encoding quantum information.

PACS numbers: 03.65.Ta, 42.50.Dv, 03.67.-a, 42.50.Ex

The dual wave-particle nature of light has been debated for centuries[1, 2]. In order to test the wave-particle duality, Wheeler proposed the famous delayed-choice gedanken experiment[3, 4]. The main experimental setup is a Mach-Zehnder interferometer. After a photon passes through the first beam splitter (BS), the choice of inserting or removing the second BS is then randomly determined. If the second BS is present, the photon travels through both beams of the Mach-Zehnder interferometer and interference fringes can be observed, indicating the wave behavior of the photon. If the second BS is absent, the photon randomly travels through one beam of the Mach-Zehnder interferometer and only one of the two output ports has a click, showing the full "which-path" information and the particle properties of the photon. Since Wheeler's proposal, many delayed-choice experiments have been realized[5–10]. All of the results support Bohr's original complementary principle[2] (classical wave-particle duality), which states that a photon may behave either as a particle or a wave, depending on the measurement setup, but the two aspects, particle and wave, appear to be incompatible and are never observed simultaneously.

Very recently, Ionicioiu and Terno proposed a quantum version of the above delayed-choice experiment, in which a quantum BS (which can be simultaneously present and absent) is utilized to replace the second BS in the Mach-Zehnder interferometer[11, 12]. In this case a continuous morphing behavior between wave and particle is expected. Soon after, several experiments were conducted, and their results confirm the morphing behavior between wave and particle[13–15]. These experiments suggest that a naive "wave or particle" description (i.e., the clas-

sical wave-particle duality) of light is inadequate and the generalization to a quantum version is necessary. In this quantum version, light exhibits particle- or wave-like behavior depending on the experimental apparatus: with a quantum detecting setup, light can simultaneously behave as a particle and as a wave, whereas with a classical setup, light behaves as a particle or as a wave[13].

In this work, by using heralded narrowband single photons, we experimentally observe the quantum wave-particle behaviors using a classical setup, the same detecting setup used in Ref.[10] to realize Wheeler's classical delayed-choice experiment. Benefiting from the long temporal length, we simultaneously and directly observe the wave and particle behaviors in a single photon's wave packet by classically inserting or removing the second BS when part of the wave packet passes through the second BS. Our results suggest that a further generalization of the aforementioned quantum wave-particle duality is necessary. One can create the superposition state of the wave and particle, and then observe its quantum behaviors with a classical detecting setup. In this aspect, the wave-particle character of the photon can be considered an additional degree of freedom, in much the same way as polarization, spin, momentum, and so on [16]. Moreover, the approach developed in our experiment is a convenient way to manipulate the wave-particle state, which has exciting potential given that the wave-particle superposition state can be used as a qubit for quantum information processing[16]. Therefore our work will not only be useful for understanding the wave-particle duality and Bohr's complementarity principle but also open up the possibility of directly using wave-particle state in encoding information.

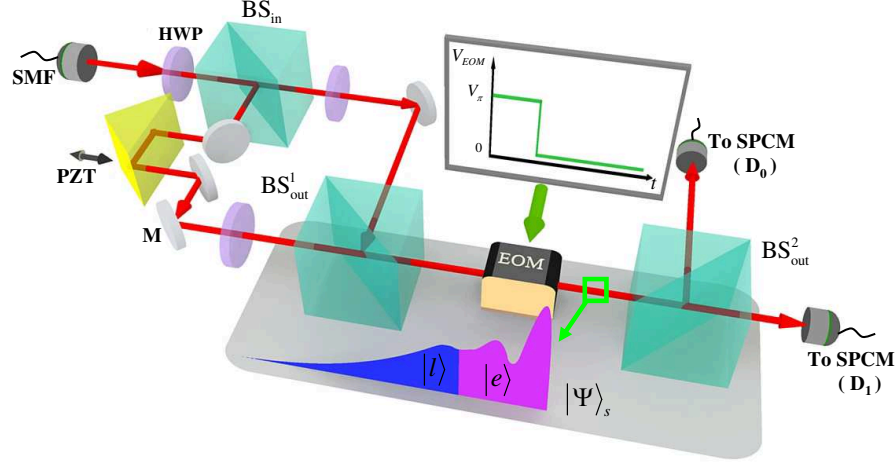


FIG. 1: Experiment setup. The main setup is a polarization beam splitter (BS) enabled Mach-Zehnder interferometer. A photon is split by BS_{in} into two modes with different orthogonal polarizations and then spatially recombined by BS_{out}^1 . An electro-optical modulator (EOM) is used as a controllable half-wave plate. BS_{out}^2 , positioned after the EOM, is used to mix the two orthogonal polarizations or split the two modes. When V_π voltage is applied to the EOM, the interference configuration is closed and the interference fringe will be detected at the two output ports. When no voltage is applied, the interferometer configuration is open, and each of the two output ports provides the full "which-path" information. Note, M: Mirror; SMF: single mode fibre; HWP: half wave plate; SPCM: single photon count module; PZT: piezo-electric transducer; $D_{0,1}$: detectors; $|e\rangle, |l\rangle$: time-bin degree states; $|\Psi\rangle_s$: single photon wave function.

Our experimental setup is shown in Fig. 1. A heralded narrowband single photon with the coherence time τ around 400 ns [17–22] is sent through a polarization BS enabled Mach-Zehnder interferometer. The detail of the heralded narrowband single photon source is described in Supplemental Material[23], which has also been described in our previous papers [22, 24]. The photon guided by a single mode fibre from the source is equally split by BS_{in} into two spatially separated paths $|0\rangle$ and $|1\rangle$ associated with orthogonal polarizations. Then the initial photon state becomes the superposition $(|0\rangle + |1\rangle)/\sqrt{2}$.

The phase shift φ between the two interferometer arms is varied by a piezoelectric transducer, resulting in the state $|\Psi\rangle = (|0\rangle + e^{i\varphi}|1\rangle)/\sqrt{2}$. Both modes are then recombined on a second controllable 'BS' (BS_{out} , see Supplemental Material[23]), which consists of two BS (BS_{out}^1 and BS_{out}^2) and an electro-optical modulator (EOM), before a final measurement in the logical $\{|0\rangle, |1\rangle\}$ basis. The inserting or removing of this controllable ' BS_{out} ' is determined when part of the narrowband photon's wave packet passes through.

Because of the long temporal length of the single narrowband photon, the time-bin degree of freedom can be well manipulated and the time-bin information can be easily detected[25–27]. We can split the photon into the time-bin superposition $|\Psi\rangle = \cos\alpha|e\rangle + e^{i\gamma}\sin\alpha|l\rangle$, where $|e\rangle$ ($|l\rangle$) is the early (late) time bin. The two modes are first overlapped by BS_{out}^1 but can still be identified by their polarization. Then the choice between closed or open interferometer configuration is achieved with the EOM: either no voltage or V_π voltage is applied to the EOM. In our experiment, V_π is applied to the EOM at the early time bin. Therefore, the BS_{out} is present and the interferometer is closed at the $|e\rangle$ time slot. In this case, the statistics of measurements at both detectors D_0 and D_1 will depend on the phase φ , which will reveal the

wave nature of the photon. Thus the photon is in the 'wave' state given by

$$|\Psi\rangle_w = |e\rangle \otimes |\psi\rangle_w, \quad |\psi\rangle_w = \cos\frac{\varphi}{2}|0\rangle - i\sin\frac{\varphi}{2}|1\rangle. \quad (1)$$

On the other hand, no voltage is applied at the late time bin and thus the controllable BS_{out} isn't present for the $|l\rangle$ time slot; hence, the interferometer is left open. In this case, both detectors will click with equal probability, which will reveal the particle nature of the photon. The photon is in the 'particle' state given by

$$|\Psi\rangle_p = |l\rangle \otimes |\psi\rangle_p, \quad |\psi\rangle_p = \frac{1}{\sqrt{2}}(|0\rangle + e^{i\varphi}|1\rangle). \quad (2)$$

Therefore, the main feature of the EOM is that it can split the single photon into two time bins and further

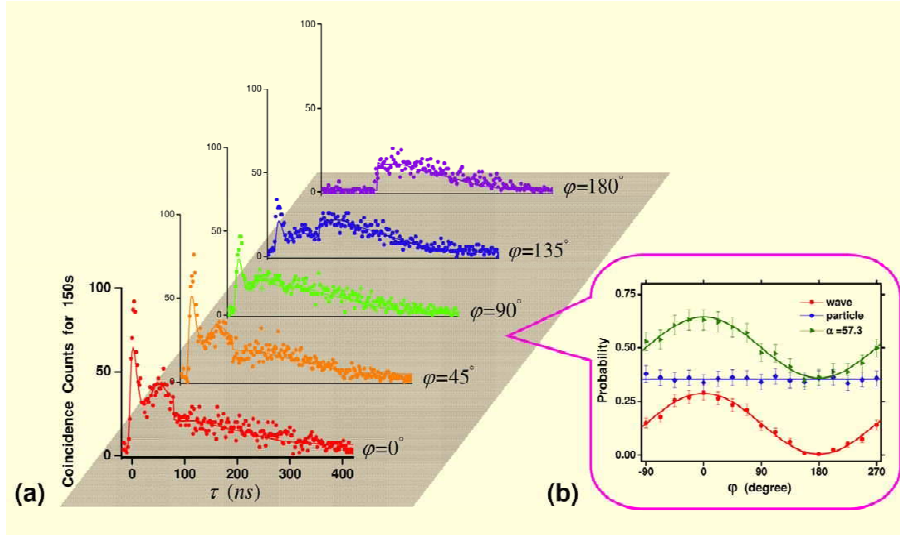


FIG. 2: Temporal wave packet of the single photon measured through coincidence counts. (a) The total temporal length of the single photon is about 400 ns. During the first 80 ns, the voltage V_π is applied to the EOM, and a clear interference fringe is observed along with the change of the phase difference φ from 0° to 180° . After 80 ns, no voltage is applied to the EOM, and the coincidence counts remain stable with different φ . (b) Probability of detecting a photon with D_0 during different time slots. The red line with filled circles stands for $0 \sim 80$ ns. The blue line with prismatic plots stands for $80 \sim 400$ ns. The green line with triangular plots stands for $0 \sim 400$ ns. For both (a) and (b), the plots and lines are experimental data and theoretical predictions, respectively.

entangle the time bin degree of freedom with the wave-particle state. For the superposition state in the time bin degree, the global state $|\Psi\rangle_s$ of the system after the EOM becomes

$$|\Psi\rangle_s(\alpha, \varphi, \gamma) = \cos \alpha |\Psi\rangle_w + e^{i\gamma} \sin \alpha |\Psi\rangle_p. \quad (3)$$

After BS_{out}^2 , we measure the photon state, and the probability of detecting the photon at detector D_0 is then given by

$$I_{D_0}(\alpha, \varphi) = \cos^2\left(\frac{\varphi}{2}\right) \cos^2 \alpha + \frac{1}{2} \sin^2 \alpha, \quad (4)$$

whereas intensity at D_1 is $I_{D_1} = 1 - I_{D_0}$.

Although the experimental setup shown in Fig.1 is the same as that in the classical delayed-choice

experiment[10], the statistics are quite different, which should be explained with the wave-particle superposition state as in the quantum delayed-choice experiment[11]. Compared with the experiment in Ref. [10], the main difference in our experiment is that a heralded single photon with long temporal length is used, thus the single photon can have three degree of freedoms: time-bin, wave-particle, and polarization. Furthermore, the time bin states $|e\rangle$ and $|l\rangle$ are entangled with the wave-particle state $|\psi\rangle_w$ and $|\psi\rangle_p$. Hence, by choosing the proper measurement basis (different time slots for $|e\rangle$ and $|l\rangle$) which can be controlled by EOM, we can demonstrate the quantum character of the wave-particle duality in this classical setup according to the above theoretical analysis.

As a typical example of experimental results, the BS_{out} is present before 80 ns and then removed at 80 ns. In this case, the α in Eq. (3) is about 57.3° , which is determined by the ratio of the coincidence counts for 0-80 ns ($|e\rangle$) and 80-400 ns ($|l\rangle$). The measured coincidence counts (time-bin 1 ns) at D_0 is shown in Fig.2(a), where φ are altered from 0° to 180° . Before BS_{out} is removed (0-80 ns), an interference fringe determined by φ is observed, which clearly reveals the wave nature of the photon. After BS_{out} is removed (80-400 ns), coincidence counts re-

main stable for all φ since only one path could be detected by D_0 , which exhibits the "which-path" information and reveals the particle nature of the photon. These results are in excellent agreement with theoretical predictions. More interestingly, the temporal wave packet of a single photon shown in Fig.2(a) demonstrates the simultaneous wave and particle behaviors. To our best knowledge, we directly observe, for the first time, the simultaneous wave and particle behaviors in one same temporal wave packet, which will shed light on further understanding of

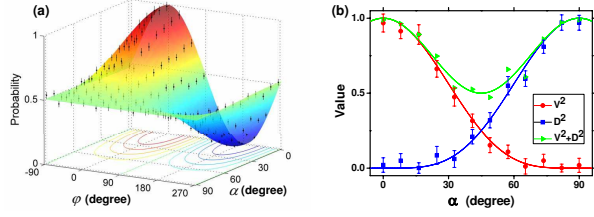


FIG. 3: Characterization of the continuous transition between wave and particle behaviors. (a) The probability of detecting a photon at D_0 as a function of the angles α and φ . Dots and error bars represent experimental data points and their corresponding standard deviations. The experimental data are fitted by using Eq.(4) and show excellent agreement with theoretical predictions. (b) Plots and related fits (solid lines) of the fringe visibility V^2 (red filled circles) and path distinguishability D^2 (blue squares) as a function of the angle α . For all angles α , the inequality $V^2 + D^2 \leq 1$ is verified.

the wave-particle duality.

The produced wave-particle supposition state can be further analyzed by choosing different measurement bases in the time bin degree. As shown in Fig. 2(b), in which data are extracted from Fig. 2(a), if $|e\rangle$ is chosen as the basis, a perfect interferometer fringe is obtained (red filled circles and line), and the interference visibility, defined as the ratio of the oscillation amplitude to the sum of the maximum and minimum probabilities, is 0.968. If $|l\rangle$ is chosen as the basis, a straight line is obtained (blue prisms and line), and the visibility is 0.043. If $|e\rangle + |l\rangle$ is chosen as the basis, a wave-particle superposition can be obtained, and the interference fringe is still observable but with a smaller visibility of 0.306 (green triangles and line). Therefore, Fig.2(b) clearly demonstrates that the visibility in the pure wave (particle) state is almost one (zero), whereas in the intermediate cases, the visibility reduces but does not vanish. This result fits very well with the theoretical prediction and has been observed in the quantum delayed-choice experiments[13].

In order to further study the features of the above wave-particle superposition state, we measure the entire coincidence counts at D_0 and then normalized (I_{D_0}) for $\alpha \in [0, 90^\circ]$ and $\varphi \in [-90^\circ, 270^\circ]$. As shown in Fig.3(a), the experimentally measured results are in excellent agreement with the theoretical predictions of Eq. (4). For the angle $\alpha = 0^\circ$, a perfect interference fringe with the visibility around one is shown as a function of φ , which corresponds to wavelike behavior. For $\alpha = 90^\circ$, the measured $I_{D_0} = 1/2$ and is independent of φ , which shows particle-like behavior. For $0^\circ < \alpha < 90^\circ$, a continuous transition from wave to particle behavior is observed, which is expressed by the continually reducing fringe visibility.

As outlined in Ref. [28–32], a generalized Bohr’s complementarity principle supports the simultaneous observation of the wave and particle behavior, but the total

wavelike and particle like information (interference fringe visibility V and path distinguishability D) should be limited by the Englert-Greenberger inequality $V^2 + D^2 \leq 1$. In our experiment, V can be obtained from the data shown in Fig.3(a), whereas $D = \frac{|N_1 - N_2|}{N_1 + N_2}$ should be measured by blocking one of the beams in the Mach-Zehnder interferometer[31]. Here N_1 is the total counts on $D_0(D_1)$ by blocking one of the beams, and N_2 is also the total counts on $D_0(D_1)$ by blocking the other beam. The results are shown in Fig.3(b), $V^2 + D^2 < 1$ when $0^\circ < \alpha < 90^\circ$, $V^2 + D^2 = 1$ only when $\alpha = 0^\circ$ or $\alpha = 90^\circ$. These results fit very well with the theoretical predictions and fulfill the Englert-Greenberger inequality for all angles of α .

Although our experimental setup is the same as the classical delayed-choice experiment in Ref.[10], the quantum behaviors as shown in Figs. 2 and 3 are clearly observed in our experiment. So our experiment suggests that a further generalization of the light’s wave-particle duality is required. Taking a spin half particle as an example, one can create a superposition state of spin up and down, and then observe the quantum behaviors of spin up and down with a classical measurement setup. Similarly, by employing the language used by Ionicioiu and Terno[11], one can write the wave function of a photon’s wave or particle state, as well as the superposition state of them. The wave-particle character of the photon can be considered an additional degree of freedom, in much the same way as polarization, spin, momentum, and so on [16]. Therefore, after creating the superposition state of the wave and particle, it is a predictable result that we can observe the simultaneous wave and particle behaviors with properly designed classical measurement setup. Thus our observation brings new meaning to the concept of wave-particle duality.

Before ending the manuscript, we briefly address that the approach developed in our experiment is a convenient way to manipulate the wave-particle state, which has exciting potential given that the wave-particle superposition state can be used as a qubit for quantum information processing[16]. In addition to that, the parameters α and φ in Eq.(3) are controllable in our experiment, and the phase γ in Eq.(3) can be manipulated too. By adding another EOM after the existing EOM, the phase γ between the wave and particle states can be tunable. In addition, with another unequal arm Mach-Zehnder interferometer, the time-bin information can be erased and the phase γ can be measured. Furthermore, by adding a $\lambda/4$ wave plate after the EOM, the wave-particle supposition can be reversed to $|\Psi\rangle_s(\alpha, \varphi, \gamma) = \cos \alpha |e\rangle |\psi\rangle_p + e^{i\gamma} \sin \alpha |l\rangle |\psi\rangle_w$.

In conclusion, we have observed the quantum wave-particle behaviors in a single photon’s wave packet with the inserting or removing of the second BS through a classical setup. The utilization of a narrowband single photon enables us to observe the wave-particle supposi-

tion state as shown in quantum delayed-choice experiments but with a classical detecting setup. The observed results will be useful in further understanding the light's wave-particle duality. Our experiment can also provide a feasible new way to create wave-particle superposition state, which could be useful in quantum information processing.

This work was supported by the NSF of China (Grants No. 11474107, 11104085, 11125417, and 61378012), the Major Research Plan of the NSF of China (Grant No. 91121023), the NFRPC (Grants No. 2011CB922104 and No. 2013CB921804), the FOYTHERG (Grant No. Yq2013050), the PRNPGZ (Grant No. 2014010), and the PCSIRT (Grant No. IRT1243). H. Yan and K. Y. Liao contributed equally to this work.

* Electronic address: yanhui@scnu.edu.cn

† Electronic address: slzhu@nju.edu.cn

- [1] J. Z. Buchwald, *The Rise of the Wave Theory of Light: Optical Theory and Experiment in the Early Nineteenth Century* (University of Chicago Press, 1989).
- [2] N. Bohr, in *Quantum Theory and Measurement* (eds Wheeler, J. A. and Zurek, W. H.) (Princeton University Press, 1984).
- [3] J. A. Wheeler, in *Mathematical Foundations of Quantum Theory* (eds Marlow, A.R.) (Academic Press, 1978).
- [4] J. A. Wheeler, in *Quantum Theory and Measurement* (eds Wheeler, J. A. and Zurek, W. H.) 182-213 (Princeton Univ. Press, 1984).
- [5] B. J. Lawson-Daku, R. Asimov, O. Gorceix, Ch. Miniatura, J. Robert, and J. Baudon, *Phys. Rev. A* **54**, 5042 (1996).
- [6] Y. H. Kim, R. Yu, S. P. Kulik, Y. Shih, and M. O. Scully, *Phys. Rev. Lett.* **84**, 1 (2000).
- [7] T. Hellmut, H. Walther, A. G. Zajonc, and W. Schleich, *Phys. Rev. A* **35**, 2532 (1987).
- [8] J. Balduhn, E. Mohler, and W. Martienssen, *Z. Phys. B* **77**, 347 (1989).
- [9] X. H. Peng, X. W. Zhu, X. M. Fang, M. Feng, M. L. Liu, and K. L. Gao, *J. Phys. A* **36**, 2555 (2003).
- [10] V. Jacques, E. Wu, F. Grosshans, F. Treussart, P. Grangier, A. Aspect, J. F. Roch., *Science* **315**, 966 (2007).
- [11] R. Ionicioiu and D. R. Terno, *Phys. Rev. Lett.* **107**, 230406 (2011).
- [12] M. Schirber, *Physics* **4**, 102 (2011).
- [13] J. S. Tang, Y. L. Li, X. Y. Xu, G. Y. Xiang, C. F. Li and G. C. Guo, *Nature Photonics* **6**, 600 (2012).
- [14] A. Peruzzo, P. Shadbolt, N. Brunner, S. Popescu, J. L. O'Brien, *Science*, **338**, 634 (2012).
- [15] F. Kaiser, T. Coudreau, P. Milman, D. B. Ostrowsky, S. Tanzilli, *Science*, **338**, 637 (2012).
- [16] G. Adesso and D. Girolami, *Nature Photonics* **6**, 579 (2012).
- [17] S. Du, P. Kolchin, C. Belthangady, G. Y. Yin, and S. E. Harris, *Phys. Rev. Lett.* **100**, 183603 (2008).
- [18] P. Kolchin, C. Belthangady, S. Du, G. Y. Yin, and S. E. Harris, *Phys. Rev. Lett.* **101**, 103601 (2008).
- [19] S. Zhang, J. F. Chen, C. Liu, M. M. T. Loy, G. K. L. Wong, and S. Du, *Phys. Rev. Lett.* **106**, 243602 (2011).
- [20] S. Zhang, C. Liu, S. Zhou, C.-S. Chu, M. M. T. Loy, and S. Du, *Phys. Rev. Lett.* **109**, 263601 (2012).
- [21] D. S. Ding, Z. Y. Zhou, B.S. Shi, and G. C. Guo, *Nat. Commun.* **4**, 3527 (2013).
- [22] K. Y. Liao, H. Yan, J. He, S. Du, Z. M. Zhang, and S. L. Zhu, *Phys. Rev. Lett.* **112**, 243602 (2014).
- [23] See Supplemental Material for the details of the heralded narrowband single photon source and the controllable 'BS'.
- [24] K. Y. Liao, H. Yan, J. Y. He, W. Huang Z. M. Zhng, and S. L. Zhu, *Chin. Phys. Lett.* **31**, 034205 (2014).
- [25] J. Brendel, N. Gisin, W. Tittel, and H. Zbinden, *Phys. Rev. Lett.* **82**, 2594 (1999).
- [26] J. M. Donohue, M. Agnew, J. Lavoie, and K. J. Resch, *Phys. Rev. Lett.* **111**, 153602 (2013).
- [27] H. Yan, S. L. Zhu, and S. W. Du, *Chin. Phys. Lett.* **28**, 070307 (2011).
- [28] B. G. Englert, *Phys. Rev. Lett.* **77**, 2154 (1996).
- [29] D. M. Greenberger and A. Yasin, *Phys. Lett. A* **128**, 391 (1988).
- [30] G. Jaeger, A. Shimony, and L. Vaidman, *Phys. Rev. A* **51**, 54 (1995).
- [31] V. Jacques, E. Wu, F. Grosshans, F. Treussart, P. Grangier, A. Aspect, and J.-F. Roch, *Phys. Rev. Lett.* **100**, 220402 (2008).
- [32] J. S. Tang, Y. L. Li, C. F. Li, and G. C. Guo, *Phys. Rev. A* **88**, 014103 (2013).

Supplemental Material for Experimental Observation of Simultaneous Wave and Particle Behaviors in a Narrowband Single Photon's Wave Packet

HERALDED NARROWBAND SINGLE PHOTON SOURCE.

Narrowband photon pairs generated through spontaneous four wave mixing and slow light technique with cold atoms are utilized to produce the heralded narrowband single photons [17] used in our experiment. The source is run periodically with a magneto-optical trap for trapping time of 4.5 ms and a biphoton generation time of 0.5 ms. The neutral ^{85}Rb atoms with an optical depth of 45 is trapped in 4.5 ms [22, 24]. A four-energy-level double- Λ system is chosen for the spontaneous four wave mixing. In the presence of the pump ($I_p \sim 50\mu\text{W}$) and coupling lasers ($I_c \sim 1.6\text{ mW}$), the counter-propagating Stokes and anti-Stokes photons are generated into opposite directions. The detecting of one Stokes photon, which also determines the start point of the experiment, heralds the generation of one narrowband single photon (anti-Stokes photon). The biphoton generation rate is 47230 s^{-1} after taking into account all of the losses. The normalized cross-correlation function $g_{s,as}^{(2)}(\tau)$ between Stokes and anti-Stokes photons is around 39, which indicates the violation of the Cauchy-Schwartz inequality by a factor of 381. The related conditional second-order correlation of the heralded single photon $g_c^{(2)} = 0.23 \pm 0.05$, which indicates a real single photon.

THE CONTROLLABLE POLARIZATION BEAM SPLITTER (BS_{out}).

In our experimental setup shown in Fig. 1, two polarization beam splitters (BS_{out}^1 and BS_{out}^2) and an electro-

optical modulator (EOM, Newport Model 4102NF) are combined into a controllable BS_{out} [10]. BS_{out}^1 combines the two beams in the Mach-Zehnder interferometer in space, but they can still be identified by their polarizations. The EOM is used as a controllable half-wave plate. The axis of the EOM is aligned 25.5° to the input polarizations. When V_π is applied to the EOM, the EOM is equivalent to a half-wave plate and can rotate the input polarization state (Horizontal and Vertical) by 45° . In this case, BS_{out}^2 after the EOM can mix the two orthogonal polarizations and erase the path information. This condition occurs when the controllable BS_{out} is present and the interferometer is closed. When $V = 0$ is applied to the EOM, the EOM has no effect on the input polarization state. In this case, BS_{out}^2 is simply used to split the two orthogonal polarizations and the path information is kept. This condition occurs when the controllable BS_{out} is absent and the interferometer is open. The EOM voltage between $V_\pi = 198\text{ V}$ and $V = 0$ can be switched via a fast MOSFET (Infineon: BSC16DN25NS3) with a switch off speed faster than 15 ns. Compared with the total 400 ns temporal length of the single photon, the maximum influence of the switch off process to the test probability is less than 0.04.